P53-10

Sympathetic Nerves in Breast Cancer: Function and In Vivo Imaging in an Orthotopic Animal Model

Kelley S. Madden[1], Mercedes J. Szpunar[2], Edward B. Brown[1]
[1]Department of Biomedical Engineering, Department of Pathology[2]
University of Rochester Medical Center, Rochester, NY USA

INTRODUCTION

Evidence from breast cancer patients and animal models of breast cancer suggests that stress can augment breast tumor growth and metastasis. Activation of the sympathetic nervous system (SNS) and release of norepinephrine (NE) from sympathetic nerves is an important stress pathway. The functional interactions between sympathetic nerves and nearby target cells have not been investigated in breast cancer.

One objective of this work is to better understand how breast tumor sympathetic nerves and NE influence tumor growth, angiogenesis, and metastasis. We use pharmacological means to reduce or elevate NE availability in 4T1 breast tumors. 4T1 is a murine breast cancer tumor model that readily grows and metastasizes in BALB/c mice. A second objective of this work is to explore the dynamic effect of catecholamine signaling on tumor vasculature using *in vivo* imaging with multiphoton laser scanning microcopy (MPLSM). To observe the relationship between sympathetic nerves and blood vessels, we have employed a transgenic mouse line in which enhanced green fluorescent protein (EGFP) expression is expressed in sympathetic tyrosine hydroxylase-positive (TH+) nerve fibers (TH-EGFP mice). Here, we use MPLSM to visualize green fluorescent nerves and blood vessels labeled with a red fluorescent molecule deep within a tumor. Ultimately, we will examine the relationship between sympathetic nerves and blood vessels as the tumor grows and in established tumors treated with antiangiogenic therapy to determine if sympathetic nerves and NE can be targeted to improve the efficacy of antiangiogenic therapy.

MATERIALS & METHODS

Cell Line. The mouse mammary adenocarcinoma line 4T1 was purchased from American Tissue Type Collection (Manassas, VA), and maintained in RPMI containing 10% FCS and penicillin/streptomycin.

Mice. Transgenic EGFP-TH mice (Swiss Webster background; Mutant Mouse Regional Resource Centers, STOCK Tg(Th-EGFP)1Gsat/Mmnc) were back-crossed to the BALB/cByJ (The Jackson Laboratory) background syngeneic for 4T1.

6-hydroxydopamine treatment. BALB/c female were injected intraperitoneally (IP) with 100 mg/kg 6-OHDA dissolved in 0.1% ascorbate in saline at d-4 and d-2 relative to 4T1 tumor cell mammary fat pad injection (orthotopic) on Day 0. Mice were injected with 50 mg/kg 6-OHDA or vehicle every 4-5 days thereafter to prevent sympathetic nerve reinnervation. 6-OHDA in adult mice does not cross the blood-brain behavior, leaving noradrenergic and dopaminergic nerve fibers in the central nervous system intact.

Desipramine (DMI) treatment. BALB/c female mice were implanted subcutaneously with a 5 mg 21-day slow release pellet (Innovative Research of America) under ketamine/xylazine anesthesia 2 days prior to 4T1 tumor cell mammary fat pad injection (Day 0).

Analysis of NE, VEGF, IL-6, and MMP-9. NE and tumor cytokines were measured in homogenates by ELISA. NE ELISA kit was purchased from Rocky Mountain Diagnostics. Mouse VEGF, IL-6, and pro-MMP-9 kits were purchased from R and D Systems, Minneapolis, MN. Results shown are based on homogenate protein concentration or tissue wet weight.

Metastasis. Lungs were harvested and submerged in formalin prior to paraffin embedding. The lobes of both lungs were sectioned into 4-µM-thick sections every 100 µM for hematoxylin and eosin (H&E) staining. Metastatic foci, visualized using a 4X objective lens by standard light microscopy, were counted in each tissue section.

Mammary tumor growth in dorsal skinfold chambers (DSC). 4T1 tumor segments, approximately 2 mm^2,4T1 mammary tumor pieces were placed on the exposed skin in a dorsal skinfold chamber surgically implanted in BALB/c EGFP-TH mice. Imaging of implanted tumors began 2 days after implant. To label blood vessels, 10 minutes before imaging, 50 µg/50 µl tetramethylrhodamine-Dextran (TMR-Dex) was injected intraorbitally in mice anesthetized with ketamine/xylazine.

Multiphoton tumor imaging. For imaging EGFP-TH+ nerve fibers, a custom-built two-photon laser-scanning microscope based upon the Fluoview 300 scanner and the BX61WI frame (Olympus America, Center Valley, PA) equipped with a MaiTai modelocked Ti:Sapphire laser (Spectra-Physics) is used. Excitation wavelength for EGFP was 920 nm and for tetramethylrhodamine (TMR) was 830 nm. EGFP fluorescence was reflected off a 565 nm long-pass dichroic, passed through a 535/40 nm filter and detected by a photomultiplier tube (Hammamatsu USA, Bridgewater, NJ). TMR fluorescence was passed through the 565 nm dichroic and a 605/30 nm filter, and detected by a photomultiplier tube. The two photon images shown here were created from a z-stack up to 120 µM in depth. Power at the sample ranged from 60-100 mW.

Statistics. Tumor growth over time was analyzed using a two-way repeated measures ANOVA. Significant main effects or interactions were analyzed using Bonferroni's post-hoc analysis. For comparing more than two groups, a significant main effect by one-way ANOVA was followed by post-hoc Neuman-Keuls analysis. For two group comparisons, Student's t-test was used. For all analyses, $p<0.05$ is considered statistically significant.

RESULTS

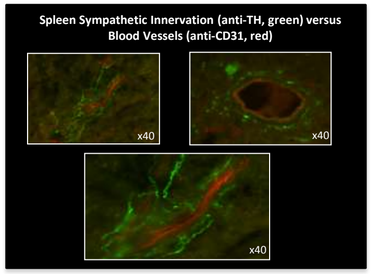

Fig. 1. Detection of sympathetic TH+ nerve fibers and CD31+ blood vessels by standard immunofluorescence in spleen. TH+ nerves (white arrows) are associated with splenic vasculature and branch into the surrounding parenchyma (white arrows).

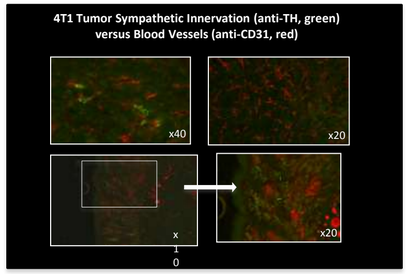

Fig. 2. Detection of sympathetic TH+ nerve fibers and CD31+ blood vessels by standard immunofluorescence in a 4T1 tumor grown in a mammary fat pad. TH+ nerves (white arrows) are often associated with blood vessels (A, C, D), except in well-vascularized areas toward the center of the tumor (B).

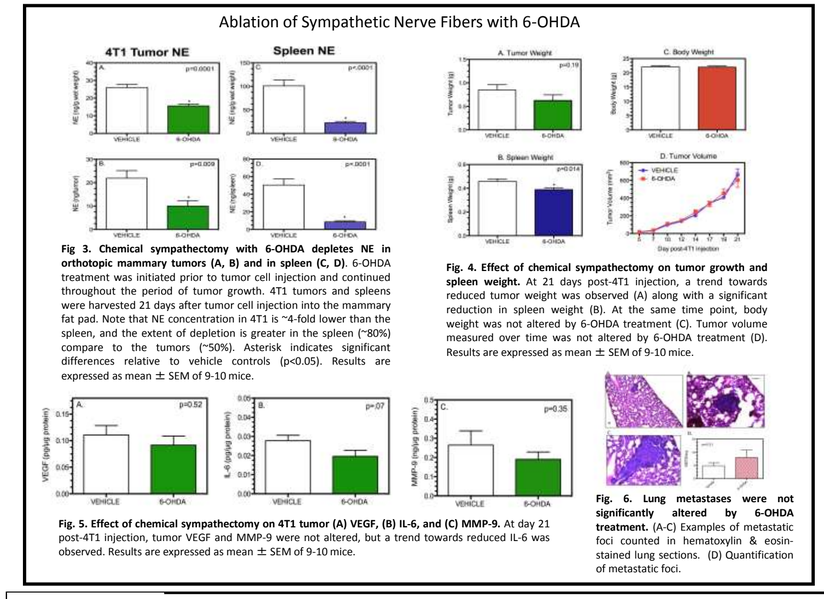

Fig 3. Chemical sympathectomy with 6-OHDA depletes NE in orthotopic mammary tumors (A, B) and in spleen (C, D). 6-OHDA treatment was initiated prior to tumor cell injection and continued throughout the period of tumor growth. 4T1 tumors and spleens were harvested 21 days after tumor cell injection into the mammary fat pad. Note that NE concentration in 4T1 is ~4-fold lower than the spleen, and the extent of depletion is greater in the spleen (~80%) compare to the tumors (~50%). Asterisk indicates significant differences relative to vehicle controls ($p<0.05$). Results are expressed as mean ± SEM of 9-10 mice.

Fig. 4. Effect of chemical sympathectomy on tumor growth and spleen weight. At 21 days post-4T1 injection, a trend towards reduced tumor weight was observed (A) along with a significant reduction in spleen weight (B). At the same time point, body weight was not altered by 6-OHDA treatment (C). Tumor volume measured over time was not altered by 6-OHDA treatment (D). Results are expressed as mean ± SEM of 9-10 mice.

Fig. 5. Effect of chemical sympathectomy on 4T1 tumor (A) VEGF, (B) IL-6, and (C) MMP-9. At day 21 post-4T1 injection, tumor VEGF and MMP-9 were not altered, but a trend towards reduced IL-6 was observed. Results are expressed as mean ± SEM of 9-10 mice.

Fig. 6. Lung metastases were not significantly altered by 6-OHDA treatment. (A-C) Examples of metastatic foci counted in hematoxylin & eosin-stained lung sections. (D) Quantification of metastatic foci.

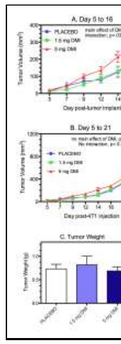

Fig. 7. DMI treatment transiently increased 4T1 tumor growth. Mice were implanted with 5 mg DMI 2 day prior to 4T1 injection. (A,B) Tumor volume was measured every 2-3 days. (C) Tumor weight was determined 21 days after 4T1 injection. Asterisks indicate significant difference vs placebo group by Bonferroni's post-hoc test ($p<0.05$). Results are expressed as mean ± SEM of n=6-7 mice per group.

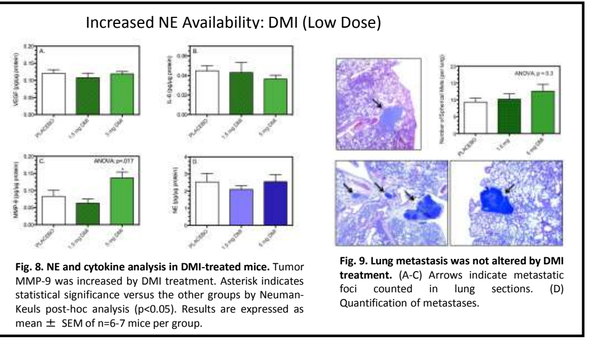

Fig. 8. NE and cytokine analysis in DMI-treated mice. Tumor MMP-9 was increased by DMI treatment. Asterisk indicates statistical significance versus the other groups by Neuman-Keuls post-hoc analysis ($p<0.05$). Results are expressed as mean ± SEM of n=6-7 mice per group.

Fig. 9. Lung metastasis was not altered by DMI treatment. (A-C) Arrows indicate metastatic foci counted in lung sections. (D) Quantification of metastases.

MPLSM Ex Vivo Imaging

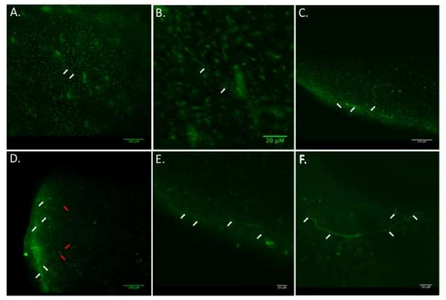

Fig. 10. MPLSM detection of TH-EGFP nerve fibers and autofluorescent cells in spleen (A,B) and orthotopic 4T1 tumor grown (C-F) in a TH-EGFP.BALB/c female mouse. EGFP+ nerve fibers were observed in spleen (A, B, arrows), but a cell-associated fluorescence was also detected that was clearly not nerve fibers. In the 4T1 tumors, nerve fibers were detected coursing through the periphery of the tumor (C-F, white arrows). In addition, single fibers were also detected as far as ~250 µM into the tumor (D, red arrows).

In Vivo Imaging by MPLSM in Dorsal Skinfold Chamber

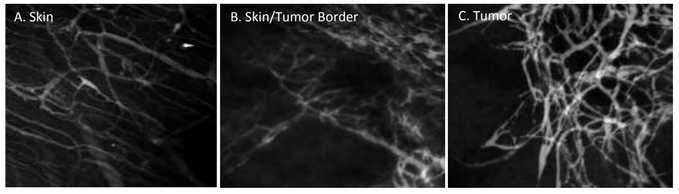

Fig 11. Blood vessels in (A) skin and (B,C) tumor growing in a dorsal skinfold chamber in a wildtype mouse. Blood vessels were labeled with tetramethylrhodamine (TMR)-dextran (2,000,000 MW). Note that blood vessels in skin are more organized and have a more consistent diameter than in tumors.

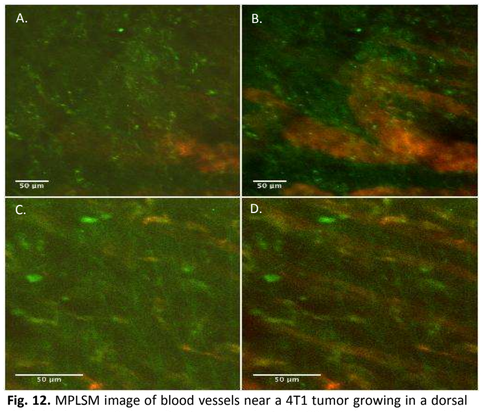

Fig. 12. MPLSM image of blood vessels near a 4T1 tumor growing in a dorsal skinfold chamber 3 days after tumor implant. (A) 39 µM deep image and (B) 246 µM deep z-projection of same region. (C) 90 µM deep and (D) 594 µM deep z-projection of same image.

SUMMARY

1. Sympathetic TH+ nerves are detected in the peripheral regions of breast tumors surrounding blood vessels and in the parenchyma of the tissue.

2. 6-OHDA, a drug that selectively abrogates sympathetic TH+ nerves, markedly depleted NE in orthotopic breast tumors.

3. Chronic NE depletion with 6-OHDA reduced breast tumor weight (trend) and significantly reduced spleen weight. Tumor MMP-9, an important prometastatic protein, was also significantly reduced by 6-OHDA treatment. However, no significant changes in lung metastases were detected.

4. Chronic DMI treatment (low dose) to increase NE availability transiently increased tumor volume. However, at the time of sacrifice, neither tumor weight or tumor volume were altered by DMI treatment. (DMI-induced increase in tumor growth has been confirmed with higher doses of DMI. See poster P53-20.)

5. Using MPLSM, we detected EGFP-expressing cells in transgenic EGFP mice in orthotopic breast tumors and spleen *ex vivo* and in tumors growing *in vivo* in a dorsal skinfold chamber. The morphology of the EGFP-expressing cells corresponded to the long TH+ nerves observed using standard immunohistochemical detection.

FUTURE PLANS

- Continue to investigate the relationship between sympathetic activation and tumor growth and metastasis.
- Use MPLSM to dynamically characterize the relationship between breast tumor blood vessels and sympathetic innervation *in vivo* in developing tumors and under a variety of treatment conditions, for example, with antiangiogenic therapy.

SUMMARY

- The majority of NE in orthotopic mammary tumors is derived from sympathetic nerve fibers.
- Ablation of sympathetic nerve fibers and depletion of NE reduced tumor growth while increased NE availability transiently increased tumor growth.
- The ability to image TH+ nerves in living mice represents an exciting technological advancement in the ability to dynamically characterize the interactions between TH+ nerves and their surrounding target cells in the growing tumor and with therapeutic treatment, such as antiangiogenic therapy.

ACKNOWLEDGEMENTS

This work was supported by Department of Defense IDEA Award (W81XWH-10-01-008) to KSM, Department of Defense Era of Hope Scholar Research Award (W81XWH-09-1-0405) to EBB, and Department of Defense Predoctoral Training Award (W81XWH-10-1-0058) to MJS. We thank Khawarl Liverpool, Giuseppi Arcuri, and Taylor Wolfgang for their excellent technical assistance.